ICAS-98-4,8,1

A98-31606

STRENGTH PREDICTION OF 2-D BRAIDED CARBON/EPOXY COMPOSITES

Dr Paul J. Falzon[1] and A/Prof Israel Herszberg[2]

[1] *Cooperative Research Centre for Advanced Composite Structures Limited, 506 Lorimer Street, Fishermens Bend, Victoria, 3207, Australia.*
[2] *Department of Aerospace Engineering, Royal Melbourne Institute of Technology, GPO Box 2476V, Melbourne, Victoria, 3001, Australia.*

ABSTRACT

Based on failure mechanisms identified from tests performed on 2-D braided composites, elementary type models which predict the strength of these materials were proposed in this paper. The formulation and numerical results generated from these models are presented. The predictions were compared with experimental data in order to validate the models. In most cases, the tension strength predictions were within 5% of measured values. The compression strength was found to be more difficult to predict with discrepancies typically under 20%. Parametric studies using the models were also performed to investigate the influence of braid angle and crimp angle on strength. It was found that the tension and compression strengths decrease with increasing braid angle. The tension strength was not influenced by the crimp angle to the same degree, while the compression strength was found to be very sensitive to the crimp angle.

INTRODUCTION

Advanced fibre reinforced composites have been successfully employed as structural materials in the aerospace industry. These composites have shown superior performance over metals in applications requiring high strength/stiffness, excellent fatigue and corrosion resistance, as well as low weight. However, the use of advanced composites has been limited by their poor resistance to impact damage and high manufacturing costs. Textile technologies provide a solution to both these problems. Well established and highly automated processes developed for the textile industry, such as braiding, have the capability to fabricate near net-shape structural preforms with the necessary fibre reinforcement to improve resistance to impact damage. Combined with a liquid moulding process, there is the potential to produce low-cost, high-quality components with improved damage tolerance. The resulting increase in design allowables, together with the cost-reducing automated manufacturing process, remove barriers from the use of composite structures for many applications. Consequently, great interest has been shown in the design, manufacture and analysis of braided composites for the aerospace industry.[1,2]

Research on modelling the elastic properties of 2-D braided composites has been extensive. Models which have been proposed can be classified into four categories: laminate theory models,[3-6] energy methods,[7,8] elementary models,[9-12] and numerical methods.[13-15] Laminate theory models have been shown to predict the in-plane elastic properties, however have drawbacks in that they are generally unable to predict the out-of-plane properties, model complex fibre architectures without over simplification, and be adapted to predict strength. Energy methods have shown to be the least used of the four model types. Although they have shown some satisfactory results, they also appear to suffer from drawbacks similar to those found with the laminate theory models. Numerical methods provide the most powerful means of analysis for braided composites. They have been employed for not only stiffness analysis, but their ability to model the fibre architecture in great detail also makes them an ideal candidate to investigate the stress/strain fields. However, the additional modelling input required, along with the increased time and effort, and the computing power necessary to perform the calculations, makes such techniques less attractive. Elementary models, which employ stiffness and compliance averaging techniques, are the simplest of the model types. Consequently, research activity falling into this category has been greatest. Elementary type models have shown to successfully predict the elastic properties of braided composites. They require less

computational effort and are able to model complex fibre architectures.

In contrast to stiffness analysis, research into strength prediction of braided composites has been scarce. A possible reason for this is the difficulty associated with such a task. An understanding of the failure mechanisms of the material is needed prior to attempting to predict the strength. This approach appears to have been ignored by most researchers.

Soebroto et al.[16,17] and Pastore & Ko[18] used a maximum strain energy criterion to predict the failure of braided composites. When the strain energy in the composite yarn exceeds the maximum strain energy, the yarn is said to fail. When a yarn fails, its contribution to the total stiffness is removed and when all yarns systems have failed then the composite is said to have failed. Fujita et al.[14,15] used a similar technique of yarn elimination to predict the fracture process of biaxial braided composites, the only difference being that stresses were used instead of strain energy. Based on the measured failure strength of glass/urethane triaxial braided composites, Dadkhah et al.[10] estimated the tensile and compressive failure stresses and strains in the axial tows. For tension, laminate theory was used to predict the stress and strain in the axial tows. While in compression, a kink band formation in the axial tows was assumed where the critical stress for kinking under uniaxial compression is related simply to the critical stress for local shear deformation.

In this paper the formulation of elementary type models which predict the strength of 2-D braided composites are presented. The models, based on findings from testing performed on 2-D braided composite specimens (which are summarised in this paper), are limited to predicting strength for two load cases: in-plane, longitudinal tension and compression. Two simplistic methods are proposed to predict the tensile strength. The first assumes the load is shared amongst the axial and bias tows, according to their respective stiffness contributions. This is referred to as the Load Sharing (LS) model. The second method assumes the load is carried entirely by the axial tows. This is referred to as the Axial Tow Only (ATO) model. A simple kink band model which relates the critical stress for local shear deformation and the tow misalignment angle (or crimp angle) to the compression stress, was used to predict the longitudinal compression strength.

Numerical results generated from the models are presented. In-plane longitudinal tension and compression tests were performed on 2-D braided specimens, with results obtained compared with the predicted values in order to validate the models. Parametric studies using the models were also performed to investigate the influence of braid angle and crimp angle on strength.

THE BRAIDING PROCESS

Braiding is basically a method which enables the interconnecting of two or more systems of yarn in the bias and longitudinal direction to form an integrated structure referred to as the preform. Due to the interconnecting nature of the yarns, braided preforms have a high level of conformability, torsional stability, and structural integrity, making them easy to handle and work with. The traditional braiding process is 2-D braiding[19] (Figure 1), which can be used to produce preforms of complex tubular shapes or in collapsed form, flat panels. The process of 2-D braiding, which has been detailed elsewhere,[19-22] can perhaps be best visualised by relating it to a "maypole dance" in which the yarns are braided over a mandrel by yarn carriers (attached to horn gears) that move in an interlinking rotational fashion around the mandrel. The resulting fibre architecture can be seen in Figure 2.

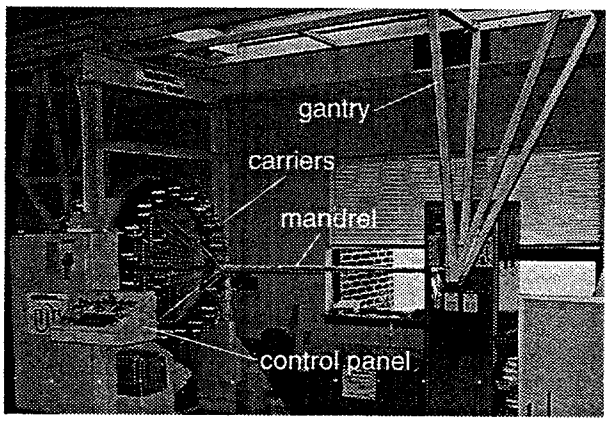

FIGURE 1 - Photograph of a 2-D braiding machine

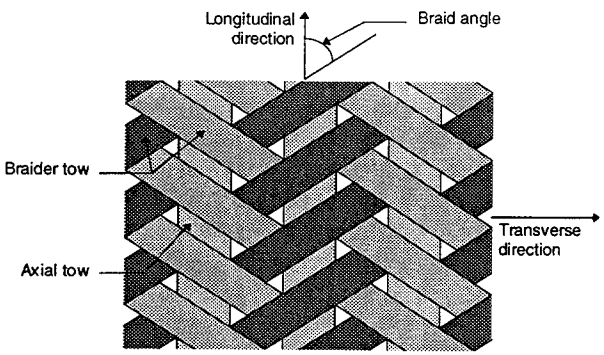

FIGURE 2 - Fibre architecture of a 2-D triaxially braided composite

MATERIALS

Figure 2 illustrates the fibre architecture of the 2-D triaxial braid used in this study. It comprises three interlaced fibre tows or yarns. Two of the tows are in the bias direction, referred to as the braider (or bias) tows which are braided in a 2 x 2 pattern. The third tow, referred to as the axial tow, is in the longitudinal direction and runs between the two braider tows. The orientation of the braider tows with respect to the axial tow is the braid angle.

A series of five different braid architectures have been considered in this study. Specimens were prepared from panels manufactured from 2-D triaxially braided preforms. The specimens tested are summarised in Table 1. The braided preforms were manufactured from 12K AS4 carbon fibre tows using a 72 carrier Wardwell braider at the Center for Composite Materials, University of Delaware. They were manufactured as a tubular preform then cut open to form a flat preform. The specimens were consolidated using Resin Transfer Moulding (RTM) with Ciba Geigy RTM6 epoxy resin system. Note that specimen types BR-45a and BR-45b have identical fibre orientations, although BR-45b was a tighter braid.

TABLE 1 - Summary of composite materials studied*

Laminate I.D.	Braid Construction	No. of plies	Percentage of 0° fibres
BR-30	0°/±30°	3	30.2
BR-45a	0°/±45°	5	26.1
BR-45b	0°/±45°	4	26.1
BR-60	0°/±60°	4	20.0
BR-LA	0°/±45°	3	41.4

* All specimens had a nominal thickness of 2.1 mm and fibre volume fraction of 60%.

EXPERIMENT

Tension Tests

The specimens used for the tension tests were based on the straight sided coupon described in ASTM D3039. In order to promote failure in the gauge section, chamfered fibreglass tabs with 22.5° taper, 40 mm long and 3 mm thick were bonded to the ends of the specimens leaving a gauge length of approximately 180 mm. To insure that a representative volume of material was tested and monitored to accurately reflect true material response, specimen widths of 30 and 38 mm were used for the various braid architectures investigated. In terms of tension testing, the standard 25.4 mm (1 inch) width was not large enough to ensure a representative failure mode.

The tabbed-ends were clamped with hydraulic grips in a servo-hydraulic testing machine and loaded to failure in stroke mode at a rate of 1.0 mm/min. Failure was defined as the first significant drop in load. Strain gauges bonded to the mid-length of specimens were used to measure the Young's modulus and Poisson's ratio.

Compression Tests

A short end-block type compression test fixture was used to measure the compression strength and stiffness. The compression specimens measured 25 mm in width and 65 mm in length. The specimens could not be as wide as the tension specimens because of size restrictions imposed by the compression test fixture. The specimens were clamped in the test fixture leaving a gauge length of 15 mm which allowed for the placement of a strain gauge in the centre of the specimen. The clamps formed part of cylindrical steel end-fittings which were guided in a steel tube comprising a viewing window. A compressive load was applied to the end fittings via a ball-and-cup arrangement. The clamps were designed so that the compressive force was transmitted predominantly by end loading.

The specimens were loaded in stroke mode at a rate of 0.5 mm/min and the tests terminated at the onset of failure. Failure was defined as the first sudden drop in load. Strain gauge readings, stroke, and loads were recorded to determine the ultimate compression strength and longitudinal compression Young's modulus of the material.

Results

Results from tests performed on braided specimens are summarised in Tables 2a and b. The stress strain response of the specimen types tested revealed that the materials behave in a linear manner up to failure. Hence, the stiffnesses were measured within the 0.05-0.5% strain range. Detailed test results can be found elsewhere.[23]

As emphasised earlier, an understanding of the failure mechanisms of the material is needed prior to proposing models which predict the strength. Consequently, observations were made on the tension and compression specimens tested. From these observations, it was postulated that the primary failure mechanism of the braided longitudinal tension specimens was transverse tension failure of the axial fibre tows. The load would then be redistributed amongst the braider tows until they failed across the tow width and

along the tow boundary until a cross-over point was reached.

TABLE 2a - Modulus, Poisson's ratio and strength values measured from longitudinal tension tests

Laminate I.D.	Modulus (GPa)	Poisson's Ratio	Strength (MPa)
BR-30	62.8 ±1.2	1.23 ±0.08	710 ±47
BR-45a	40.4 ±0.8	0.75 ±0.02	451 ±15
BR-45b	41.4 ±0.5	0.73 ±0.01	458 ±42
BR-60	30.9 ±0.9	0.34 ±0.01	333 ±10
BR-LA	56.3 ±1.3	0.63 ±0.08	703 ±33

N.B.: mean value ±standard deviation

TABLE 2b - Modulus and strength values measured from compression tests

Laminate I.D.	Modulus (GPa)	Strength (MPa)
BR-45a	32.8 ±0.9	284 ±48
BR-45b	34.3 ±2.0	332 ±23
BR-60	28.0 ±2.0	270 ±40
BR-LA	50.4 ±5.2	355 ±29

For the braided longitudinal compression specimens, the primary failure mechanism was identified as transverse shear resulting from kink band formation in the axial tows. It has been suggested that fibres which are not aligned with the load direction will form a failure nucleus that undergoes kinking, which occurs at a stress lower than the ideal micro-buckling strength.[24] This is the case with the braided specimens, where undulations exist in the axial tows (Figure 5).

STRENGTH PREDICTION MODELS

Tension Model Theory

Longitudinal tension tests performed on braided composites, as detailed earlier, revealed failure occurred in the axial tows through transverse tension, with minimal damage to the bias fibre tows. This indicates that the majority of the load is carried by the axial tows. If the quantity of load carried by the axial tows can be predicted, then the longitudinal tension strength of the braided composite can be calculated using a simple maximum stress failure criterion.

As explained earlier, two methods are proposed to estimate the load carried by the axial tows. The first assumes the load is shared amongst the axial and bias tows (Load Sharing (LS) model), while the second model assumes that the load is carried entirely by the axial tows (Axial Tow Only (ATO) model).

Load Sharing Model

Assuming the braided composite follows the linear elastic law in longitudinal tension, then the tension stress in the composite, σ_t, can be expressed as,

$$\sigma_t = E_t \times \varepsilon \quad (1)$$

where,

E_t = composite longitudinal tension modulus
ε = average strain in the composite

If it is assumed that the load carried by the axial tow is in proportion to its stiffness contribution, the longitudinal tension stress in the axial tow, σ_t^a, can be calculated similarly to Equation (1) as follows,

$$\sigma_t^a = E_t^a \times \varepsilon \quad (2)$$

where,

E_t^a = axial tow longitudinal tension modulus

Approximating the axial tow longitudinal tension stiffness and strength by the following expressions,

$$E_t^a = E_f^a \times V_f \quad (3)$$

where,

E_f^a = axial tow fibre longitudinal modulus
V_f = fibre volume fraction of braided composite

and substituting Equations (2) and (3) into Equation (1), then the longitudinal tension stress in the braided composite can be expressed in terms of the axial tow stress and stiffness ratio as follows,

$$\sigma_t = \sigma_t^a \times \frac{E_t}{E_f^a . V_f} \quad (4)$$

Using a maximum stress failure criterion, the ultimate longitudinal tension strength of the braided composite, $\sigma_t^{ult.}$, occurs when the stress in the axial tow reaches its ultimate strength. Approximating the axial tow ultimate strength, $\sigma_{t,ult.}^a$, as follows,

$$\sigma_{t,ult.}^a = \sigma_f^a \times V_f \quad (5)$$

where,

σ_f^a = axial tow fibre longitudinal strength

then $\sigma_t^{ult.}$ can be calculated by the following expression,

$$\sigma_t^{ult.} = \sigma_f^a \times \frac{E_t}{E_f^a} \quad (6)$$

Axial Tow Only Model

Assuming that the entire load is carried by the axial tows, then for a given applied longitudinal tension load, the resulting longitudinal tension stress in the braided composite, σ_t, can be expressed in terms of the stress in the axial tow, σ_t^a, as follows,

$$\sigma_t = \sigma_t^a \times v_a \quad (7)$$

where,

v_a = volume fraction of axial tows

Using a maximum stress failure criterion, the ultimate longitudinal tension strength of the braided composite, $\sigma_t^{ult.}$, occurs when the stress in the axial tow reaches its ultimate strength. So, using Equation (5) along with Equation (7), $\sigma_t^{ult.}$ can be calculated by the following expression,

$$\sigma_t^{ult.} = \sigma_f^a \times v_a \times V_f \quad (8)$$

Compression Model Theory

As identified from experiment, the longitudinal compression failure of the braided composites studied was driven by kink band formation in the axial tows. The mechanics associated with kink band formation is well understood. For polymer composites, the critical stress for kinking under uniaxial compression, σ_k, can be related simply to the critical stress for local shear deformation, τ_0, and the angle of misalignment with respect to the applied load (or fibre crimp angle), ξ. The relationship can be expressed as follows:[10]

$$\sigma_k = \frac{\tau_0}{\xi} \quad (9)$$

The value of σ_k predicted by Equation (9) is the stress in the axial tows at peak load, $\sigma_{c,ult.}^a$.

If a pure strain condition is assumed then the stress in the braided composite, σ_c, can be related to the stress in the axial tow, σ_c^a, as follows,

$$\sigma_c = \sigma_c^a \frac{E_c}{E_c^a} \quad (10)$$

where,

E_c = composite longitudinal compression modulus
E_c^a = axial tow longitudinal compression modulus

Approximating the axial tow longitudinal stiffness by the following expression,

$$E_c^a = E_f^a \times V_f \quad (11)$$

and substituting Equations (9) and (11) into Equation (10), than the longitudinal compression strength of the braided composite, $\sigma_c^{ult.}$, can be calculated as follows,

$$\sigma_c^{ult.} = \frac{\tau_0}{\xi} \times \frac{E_c}{E_f^a . V_f} \quad (12)$$

ANALYSIS OF BRAIDS

The braid architectures described earlier were analysed using the aforementioned strength models to predict their longitudinal tension and compression strengths. The fibre tow properties used in the calculations were obtained from tension tests performed on impregnated carbon fibre tows. Details of these tests are given elsewhere.[23] Predicted and measured elastic properties of the braided composites were also used. Measured values were obtained from the tension and compression tests discussed earlier, while predicted values were calculated using stiffness averaging techniques which are detailed elsewhere.[25] A value of 75 MPa was used as the critical stress for local shear deformation. Values typically range between 70 and 80 MPa for aerospace grade resins.[10] A summary of the material property input is given in Table 3. The strength predictions are shown graphically in Figures 3 and 4.

TABLE 3 - Material property input used in the strength modelling

Axial fibre tow long'l modulus, E_f^a	230 GPa
Axial fibre tow long'l strength, σ_f^a	2.89 GPa
Critical stress for local shear def'n, τ_0	75 MPa

Tension

Firstly looking at the longitudinal tension strength (Figure 3), it can be seen that the correlation between the predicted and measured values is good, particularly when the scatter in the measured data is taken into account. Two sets of predictions were calculated with the LS model.

Those using the predicted longitudinal tension modulus and those using the measured modulus. Of the two predictions, those using the measured modulus compare best with the measured values, although both over estimated the strength. This highlights a disadvantage of the LS model in that it is dependent on an accuracy of the tension modulus of the material. Any discrepancies which may exist in predicting the stiffness will also be included in the strength prediction.

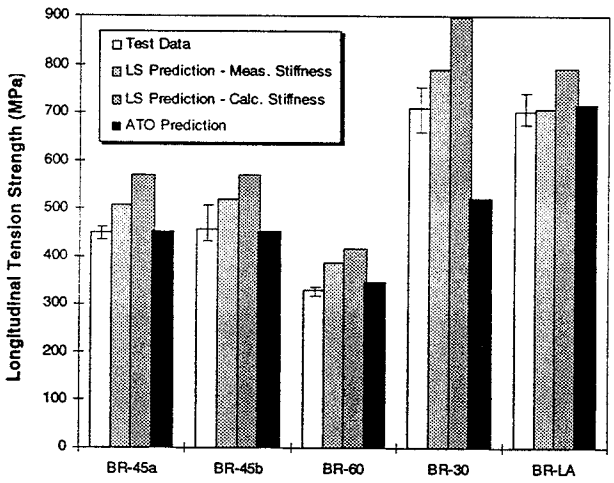

FIGURE 3 - Longitudinal tension strength predicted by the load sharing (LS) and axial tow only (ATO) models for various braid architectures compared with test data

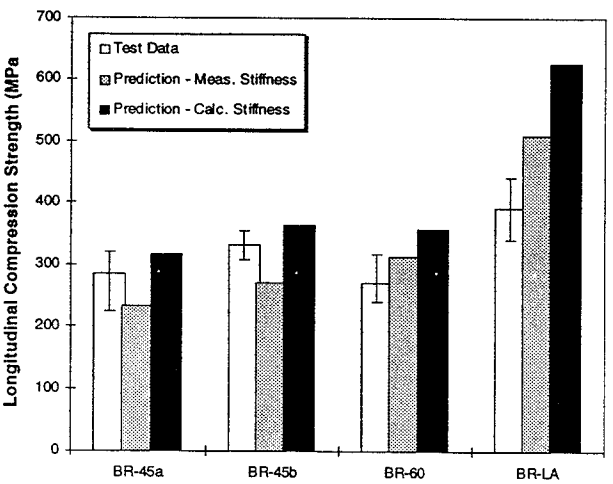

FIGURE 4 - Longitudinal compression strength predicted by the kink band model compared with test data

The predictions using the ATO model generally compared better to the measured data than did the LS predictions. In most cases, the ATO predictions are within 5% of the measured strengths. The only exception being the BR-30 specimen, where the difference is around 25%. In contrast, the LS predictions are more accurate with specimens which have a higher proportion of 0° reinforcement or smaller braid angle (specimens BR-30 and BR-LA).

The reason for the observed differences in the model predictions may be attributed to the shear occurring in the bias yarns as a result of the longitudinal tension load. Although the axial yarns are loaded in tension, the load carried by the bias yarns occurs through a shear mechanism. Therefore, the proportion of load carried by the bias yarns is dependent on three parameters; the shear stiffness of the fibres; the proportion of bias yarns; and the off-axis angle of the yarns. Due to the nonlinear behaviour of the shear modulus for a given carbon/epoxy tow, as the load is increased the shear stiffness decreases, thus reducing the load carrying capacity of the fibres. Therefore, it is hypothesised that as the braided composite approaches failure, the load carrying capacity of the bias yarns is diminished, resulting in almost all the load being carried by the axial tows. For braids with smaller braid angles the extent to which the load carrying capacity of the bias yarns drops is less, and so the load is still shared amongst the axial and bias tows when failure occurs. Similarly, for braids with a high proportion of axial fibres the influence the bias tows have on the overall behaviour of the material is less, and the assumption that the load is shared is more accurate.

From these limited observations, it may be concluded that the ATO model is better suited to braid architectures with angles larger than 40°, while the LS model is more suited to braids with angles less than 40° and axial tow reinforcements in excess of 40%.

Compression

Comparisons between predicted and measured longitudinal compression strengths are shown in Figure 4. The value used in the calculations for the tow misalignment angle, ξ, for each of the braid types was the average axial tow crimp angle (Table 4). These angles were measured from micrographs of through-thickness cross-sections of the braided composites studied. Further details of this work can be found elsewhere.[25] A typical micrograph showing the axial tow crimp can be seen in Figure 5.

As with the LS model, two sets of predictions were calculated with the compression strength model. Those using the predicted longitudinal compression modulus, which is identical to the longitudinal tension modulus, and those using the measured compression modulus. Of the two

predictions, those using the measured modulus compared better overall, with differences less than 20% in most cases. Although the predictions using the calculated modulus, which over estimated the strength in all cases, compared better for the BR-45a and BR-45b specimens, with discrepancies around 10%. Overall, the comparisons are reasonable, particularly when the scatter in the measured strengths is taken into consideration.

TABLE 4 - Summary of average crimp angles

Specimen	Crimp Angle
BR-30	3.3°
BR-45a	4.5°
BR-45b	3.9°
BR-60	2.9°
BR-LA	3.1°

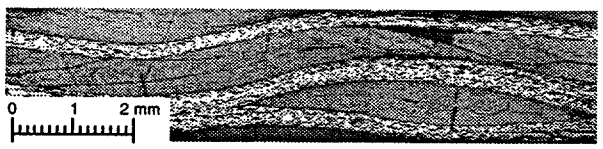

FIGURE 5 - Photomicrograph of a braided composite showing crimp of the axial fibre tows

The reasons for the discrepancies may be attributed to two factors. Firstly, it is assumed that all the specimens fail through pure compression failure with no specimen instability through buckling. Buckling of the specimen would cause a lower compression strength, and thus result in an over estimation of the strength, as has generally occurred. Secondly, the analysis can be shown to be highly sensitive to the value used for the tow misalignment angle. As can be seen in Figure 6, the predicted strength can vary dramatically with small variations in the misalignment angle. This is especially the case with small crimp angles, typical with those measured and used in the analysis. This sensitivity makes it difficult to predict the strength accurately. It should be kept in mind that the average crimp angle was used as the tow misalignment angle. In reality, the specimen would fail at a weak point, which would likely occur where the crimp angle is larger than the average value used. This is in line with the fact that the analysis generally over estimates the compression strength. A larger tow misalignment angle would reduce the predicted strength.

Parametric Study of Braids

A parametric study was performed to investigate the variation of longitudinal tension and compression strength with braid angle and crimp angle. These calculations were performed assuming a fibre volume fraction of 60% and the axial and braider tows being of the same material (AS4 carbon) and yarn size (12 K). The ratio of braider to axial tows used was 2 to 1.

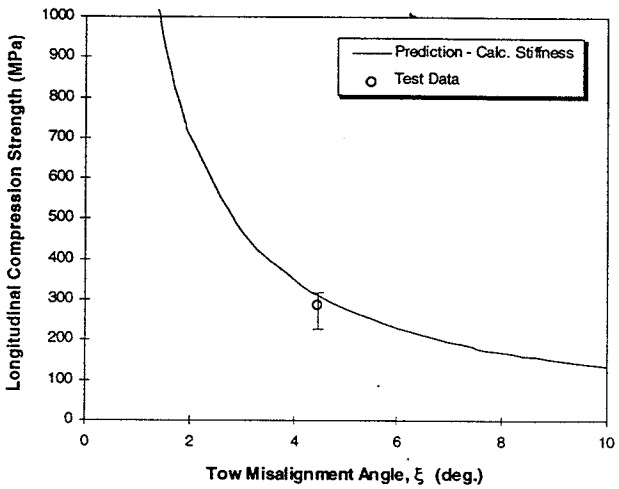

FIGURE 6 - Variation of predicted longitudinal compression strength with tow misalignment angle for the BR-45a braid.

Variation with Braid Angle

Figures 7 and 8 show the variation of longitudinal tension and compression strength with braid angle. The symbols on the graphs indicate the test results which were presented earlier. In the case of the tension strength (Figure 7), the combination of the two models (ATO and LS) predict the changes in the strength quite well. For braid angles less than 40° the trend follows the LS model, while beyond 40°, the trend follows the ATO model. In actual fact, the trend is almost identical for both the LS and ATO models beyond a braid angle of 50°, although the ATO model provides a more accurate prediction. Looking at the trend further, it can be seen as the braid angle increases from 20° to 80°, the LS model predicts a decrease in the longitudinal tension strength by some 80% (Figure 7). This reduction in strength is attributed to the decrease in axial fibre content which occurs when the braid angle increases.

The trend predicted by the LS model for tension strength is very similar to that predicted by the kink band model for compression strength (Figure 8). Based on the range of average crimp angles measured from the braided composite studied, two tow misalignment angles were used in the calculations, ξ = 3° and 5°. Irrespective of the misalignment angle, the trends predicted are similar and coincide reasonably well with the limited measured data. As the braid angle increases from 20° to 80°, it can be seen that the kink band model predicts a decrease in the

longitudinal compression strength by also some 80% (Figure 8). This coincides with the decrease in tension strength, and can be explained by the same reasoning.

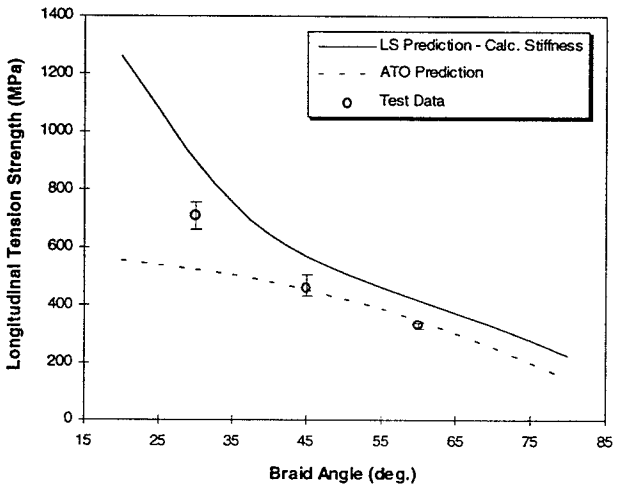

FIGURE 7 - Variation of predicted longitudinal tension strength with braid angle

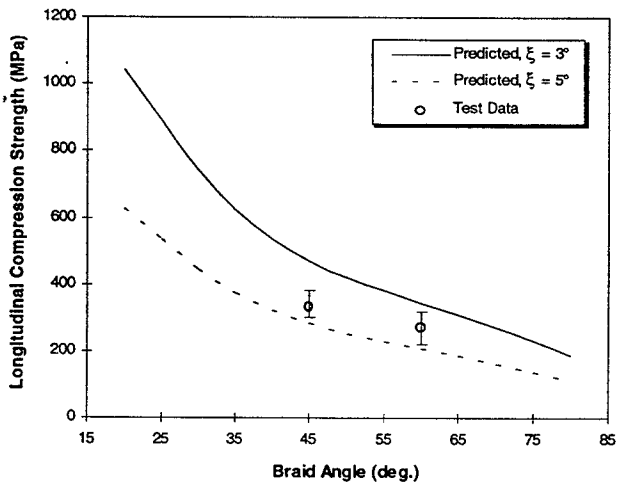

FIGURE 8 - Variation of predicted longitudinal compression strength (using calculated stiffness) with braid angle

The trends identified in Figures 7 and 8 were compared with trends found by Naik.[26] Naik predicted the strength to drop by 15% with a change of braid angle from 63° to 72°. This is consistent with the findings using the LS and ATO models. This sensitivity of longitudinal tension and compression strength with braid angle can strongly influence variability in the mechanical performance of braided composites. For example, by considering a 0/±45° braid, varying the braid angle by ±2.5° causes the longitudinal tension and compression strengths to each change by 6%. This sensitivity may also be a reason for discrepancies that exist between experimental data and model predictions.

Variation with Crimp Angle

The influence of crimp angle on the longitudinal tension and compression strengths is shown in Figures 9 and 10 respectively. The symbols on the graphs indicate the test results which were presented earlier. The braid architecture considered in this study was a 0/±45° triaxial braid represented by specimen type BR-45a. As can be seen in Figure 9, the ATO model is independent of crimp angle and so there is no variation of the predicted longitudinal tension strength with crimp angle. With the LS model, there is a small decrease in the tension strength as the crimp angle increases from 0° to 10°. It is not until the crimp angle exceeds 10° that the tension strength undergoes any substantial change. The tension strength drops by 20% when the crimp angle is 20°. Naik[26] found similar trends relating tension strength and crimp angle. For different braid architectures, Naik predicted small strength reductions for crimp angles below 7°, however the strength was reduced by up to 30% for crimp angles reaching 20°. For the typical crimp angles which were measured from the braided specimens studied, the LS model predictions indicate that the longitudinal tension strength is not extremely sensitive to fibre crimp.

In contrast to the tension strength, the longitudinal compression strength is highly sensitive to the crimp angle, especially in the first 5° to 10° (Figure 10). This sensitivity was highlighted earlier in Figure 6 which shows the variation of compression strength with tow misalignment angle.

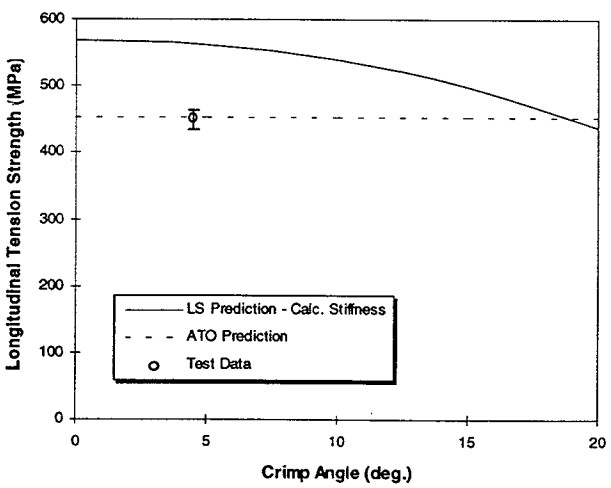

FIGURE 9 - Variation of predicted longitudinal tension strength with crimp angle for the BR-45a braid

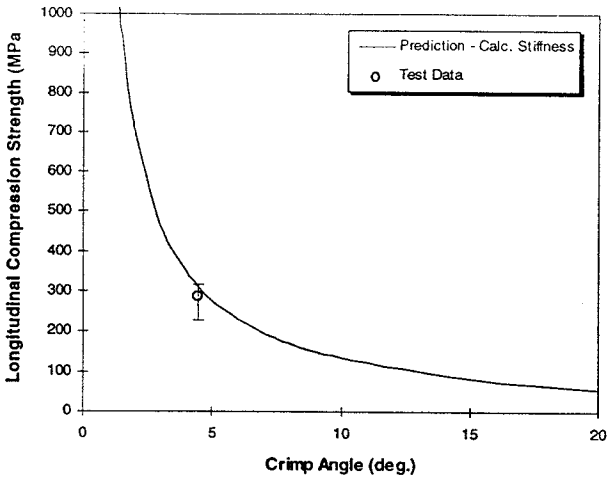

FIGURE 10 - Variation of predicted longitudinal compression strength with crimp angle for the BR-45a braid.

CONCLUSIONS

Based on failure mechanisms identified from tests performed on 2-D braided composites, elementary type models which predict the strength of these materials were proposed. Two simple techniques were developed to predict the longitudinal tension strength. The first assumed that the load was shared amongst the axial and bias tows, and was referred to as the Load Sharing (LS) model. The second method assumed the load was carried entirely by the axial tows and was referred to as the Axial Tow Only (ATO) model. Comparisons made between experimental data and predictions using the two models revealed that the ATO model generally compared better to the measured data, than did the LS model. In most cases, the ATO predictions were within 5% of the measured strength. The LS predictions were more accurate for specimens with a higher proportion of 0° reinforcement or smaller braid angle

A kink band model, which related the critical stress for local shear deformation and the tow misalignment angle to the compression stress, was developed to predict the longitudinal compression strength. Comparisons with experimental data revealed that the compression strength was more difficult to predict, with discrepancies typically under 20%. The major problem with the analysis is the sensitivity of the calculations to the tow misalignment angle, which was difficult to predict.

Parametric studies were performed using the tension and compression strength models. The tension and compression strengths were found to decrease with increasing braid angle. The tension strength was not influenced by the crimp angle to the same degree, while the compression strength was found to be very sensitive to the crimp angle.

REFERENCES

(1) Jackson, A.C., Barrie, R.E., Shah, B.M. and Shukla, J.G., Advanced Textile Applications for Primary Aircraft Structures, *NASA CP 3154, Second NASA Advanced Composites Technology Conference, November 4-7, 1991, pp.325-353.*

(2) Fedro, M. J. and Willden, K., Characterization and Manufacture of Braided Composites for Large Commercial Aircraft Structures, *NASA CP 3154, 1991, pp.387-429.*

(3) Yang, J.-M., Ma, C.-L. and Chou, T.-W., Fiber Inclination Model of Three-Dimensional Textile Structural Composites, *Journal of Composite Materials, Vol.20, September 1986, pp.472-484.*

(4) Byun, J.-H., Whitney, T. J., Du, G.-W. and Chou, T.-W., Analytical Characterisation of Two-Step Braided Composites, *Journal of Composite Materials, Vol.25, Dec. 1991, pp.1599-1618.*

(5) Yang, J.-M. and Chou, T.-W., Thermo-Elastic Analysis of Three Dimensional Fabric Composites, *Advances in Aerospace Science and Engineering, ASME 1984, pp.61-68.*

(6) Redman, C.J. and Douglas, C.D., Theoretical Prediction of the Tensile Elastic Properties of Braided Composites, *38th International SAMPE Symposium, May 10-13, 1993, pp.719-727.*

(7) Hearle, J.W.S., Micro- and Macro-Mechanics of Textile Fabrics, Advances in Composite Materials and Structures, *Presented at The Winter Annual Meeting of the ASME, December 1986, American Society of Mechanical Engineers, 1989, pp.131-134.*

(8) Ma, C.-L., Yang, J.-M. and Chou, T.-W., Elastic Stiffness of Three-Dimensional Braided Textile Structural Composites, *Composite Materials: Testing and Design (Seventh Conference), April 2-4, 1984, ASTM STP 893, American Society for Testing and Materials, Philadelphia, 1986, pp.404-421.*

(9) Jaranson, J., Pastore, C., Singletary, J., Field, S., Kharod, A.M., Kniveton, T. and Rushing, T., Elastic Properties of Triaxially Braided Glass/Urethane Composites, *Advanced Composites Techniques: Proceedings of the 9th*

Annual ASM/ESD Advanced Composites Conference, November 8-11, 1993, pp.359-377.

(10) Dadkhah, M.S., Flintoff, J.G. and Cox, B.N., Simple Models for Triaxially Braided Composites, *Composites, Vol.26, 1995, pp.561-577.*

(11) Naik, R.V., Ifju, P.G. and Masters, J.E., Effect of Fiber Architecture Parameters on Deformation Fields and Elastic Moduli of 2-D Braided Composites, *Journal of Composite Materials, Vol.28 No.7, 1994, pp.656-681.*

(12) Naik, R.A., Analysis of Woven and Braided Fabric Reinforced Composites, *NASA CR 194930, NASA Langley Research Center, June 1994.*

(13) Masters, J.E., Foye, R.L., Pastore, C.M. and Gowayed, Y.A., Mechanical Properties of Triaxially Braided Composites: Experimental and Analytical Results, *NASA Contractor Report 189572, Contract NAS1-19000, January 1992.*

(14) Fujita, A., Maekawa, Z., Hamada, H. and Yokoyama, A., Mechanical Behavior and Fracture Mechanism in Flat Braided Composites. Part 1: Braided Flat Bar, *Journal of Reinforced Plastics and Composites, Vol.11, June 1992, pp.600-617.*

(15) Fujita, A., Maekawa, Z., Hamada, H. and Yokoyama, A., Mechanical Behavior and Fracture Mechanism in Flat Braided Composites. Part 2: Braided Flat Bar with a Circular Hole, *Journal of Reinforced Plastics and Composites, Vol.11, June 1992, pp.618-632.*

(16) Soebroto, H.B., Hager, T. and Pastore, C.M., Engineering Design of Braided Structural Fiberglas Composites, *35th International SAMPE Symposium, April 2-5, 1990, pp.687-696.*

(17) Soebroto, H.B., Pastore, C.M. and Ko, F.K., Engineering Design of Braided Structural Fiberglas Composite, *Structural Composites - Design and Processing Technologies, October 1990, pp.435-440.*

(18) Pastore, C.M. and Ko, F.K., A Processing Science Model for Three Dimensional Braiding, *Proceedings of the 4th Annual Conference on Advanced Composites, Sept.13-15, 1988, ASM International, Ohio, 1988, pp.371-376.*

(19) Brunnschweiler, D., Braids and Braiding, *Journal of the Textile Institute, Vol.45, 1954, pp.P666-686.*

(20) Ko, F.K., Pastore, C.M. and Head, A.A., Handbook of Industrial Braiding, *Atkins & Pearce, 1989.*

(21) Ko, F.K., Braiding, *Engineering Materials Handbook Vol.1, ASM International, 1987, pp.519-528.*

(22) Popper, P., Braiding, *International Encyclopaedia of Composites, S. Lee ed., VCH Publishers Inc., Vol.1, pp.130-147.*

(23) Falzon, P.J. and Herszberg, I., Mechanical Performance of 2-D Braided Carbon/Epoxy Composites, *to be published in Composites Science and Technology, 1998.*

(24) Camponeschi, E.T., Jr., Compression of Composite Materials: A Review, *Composite Materials: Fatigue and Fracture (Third Volume), ASTM STP 1110, 1991, pp.550-578.*

(25) Falzon, P.J., The Design, Manufacture and Performance of Two-Dimensional Braided Composites, *PhD Thesis, Royal Melbourne Institute of Technology, 1997.*

(26) Naik, R.A., Failure Analysis of Woven and Braided Fabric Reinforced Composites, *NASA Contractor Report 194981, September 1994.*